Supplementary Material

The columnar and laminar organization of inhibitory connections to neocortical excitatory cells

Dennis Kätzel[1], Boris V. Zemelman[2], Christina Buetfering[1], Markus Wölfel[2], and Gero Miesenböck[1,2]

[1] Department of Physiology, Anatomy and Genetics, University of Oxford, Parks Road, Oxford, OX1 3PT, UK

[2] Department of Cell Biology, Yale University School of Medicine, 333 Cedar Street, New Haven, CT 06520, USA

SUPPLEMENTARY FIGURES

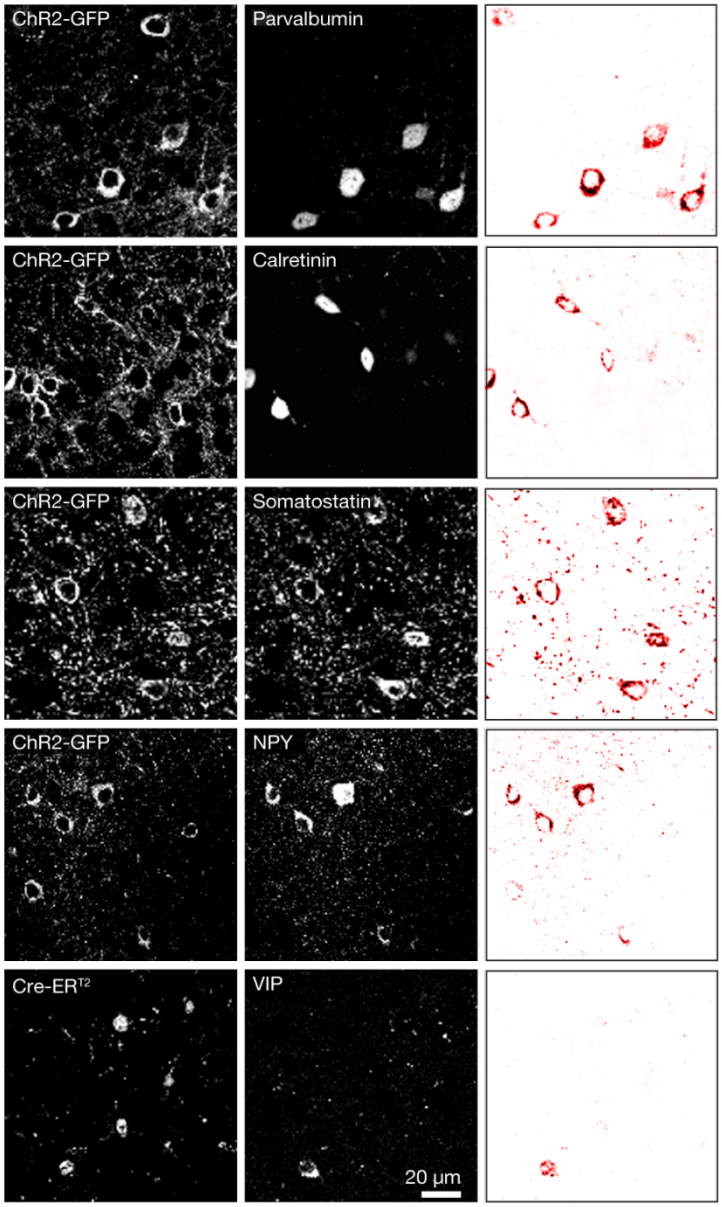

Supplementary Figure 1. Cell-type specificity of ChR2-EGFP expression. Neocortical slices were obtained from *Gad2::Cre-ER^{T2} R26::ChR2-EGFP* mice 1–7 days after tamoxifen induction and immunolabeled. The left and center columns show raw confocal images after staining with fluorescently labeled secondary antibodies; the right column displays the corresponding colocalization maps, which were produced by multiplying the two fluorescence channels on a pixel-by-pixel basis and normalizing the resulting product image to 8 bits. ChR2-EGFP expression is detected in all major interneuron subclasses, which are defined by the expression of calcium binding proteins and neuropeptides. See Supplementary Table 1 for summary statistics.

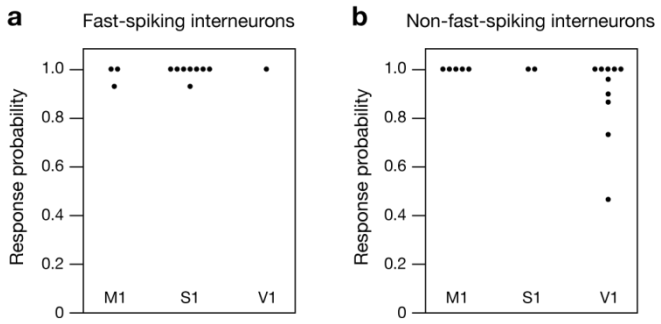

Supplementary Figure 2. Responsiveness of interneurons to optical stimulation. Spiking probabilities were estimated by stimulating neocortical interneurons in layer 5B of M1, S1, and V1 with a sequence of 30 light pulses (473 nm, 20 ms pulses, 2.0 mW of optical power, 0.2 Hz). Each data point represents one cell. Three criteria were used to distinguish fast- from non-fast-spiking neurons: fast-spiking neurons *i*) attained firing rates > 100 Hz during a 500-ms depolarizing current step of 300 pA; *ii*) exhibited a ratio > 0.7 of the average interspike interval (ISI) at the beginning and end of the depolarizing current step (averages of 3 ISIs each); and *iii*) displayed a spike width of ≤ 1ms at half-maximal amplitude. Cells that met all three criteria were classified as fast-spiking (**a**); cells that failed all three criteria as non-fast-spiking (**b**). Six neurons were excluded because they met some but not all criteria; four neurons were unresponsive to light. No significant differences in the responsiveness of fast- and non-fast-spiking interneurons in different cortical areas were detected by parametric one-way ANOVA ($P = 0.704$ and 0.235 for fast- and non-fast-spiking cells, respectively).

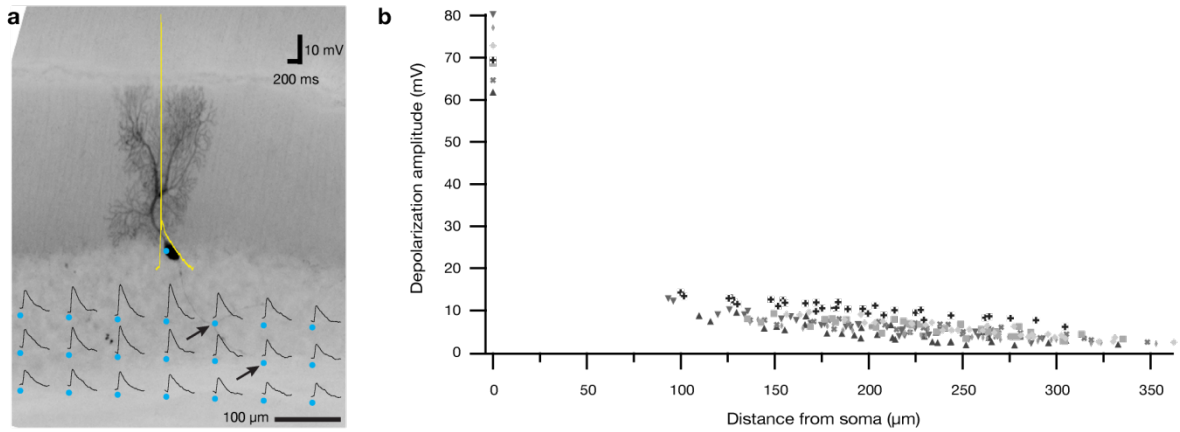

Supplementary Figure 3. Perisomatic but not axonal photostimulation evokes action potentials. To examine the possibility of eliciting action potentials by axonal photostimulation, GABAergic Purkinje cells, which possess anatomically well-separated dendritic and axonal compartments, were analyzed in cerebellar slices obtained from *Gad2::Cre-ER*^{T2} *R26::ChR2-EGFP* mice 1–7 days after tamoxifen induction. (**a**) In the representative example shown, optical raster stimulation of cerebellar white matter (blue dots; 20-ms pulses of 0.5 mW optical power) fails to elicit backpropagating action potentials in a Purkinje cell under current clamp (native resting potential –68 mV), even when the stimulating laser beam directly overlaps the axon of the recorded cell (arrows). Somatic stimulation reliably elicits spiking (yellow trace). (**b**) The amplitudes of light-evoked depolarizations as a function of the distance of the focused stimulation beam from the soma ($n = 7$ Purkinje cells, represented with different symbols). All data points follow a linear trend without stimulation hotspots, demonstrating the absence of direct axonal stimulation.

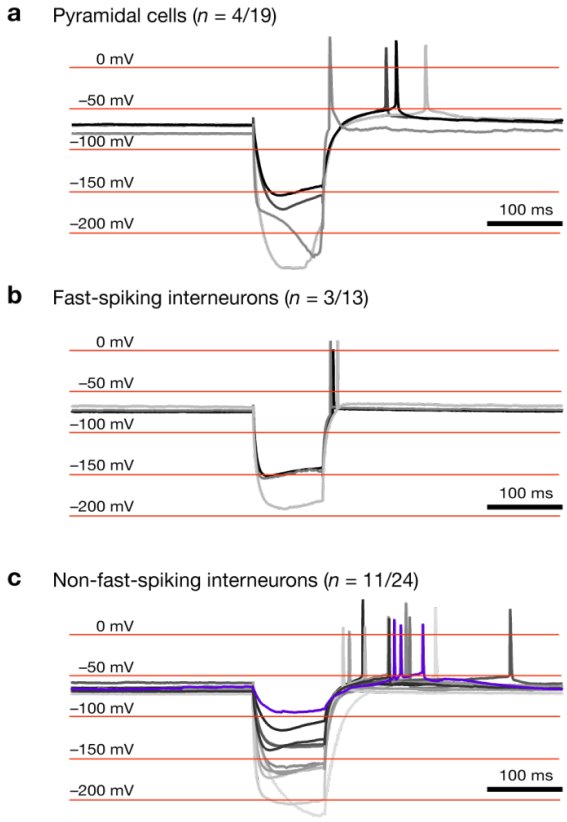

Supplementary Figure 4. Rebound spiking requires strong hyperpolarization. To define the requirements for eliciting rebound spikes, hyperpolarizing 100-ms current steps of increasing amplitudes (maxima between –200 and -–1100 pA) were injected into (**a**) neocortical pyramidal cells (n = 19 cells), (**b**) fast-spiking interneurons (n = 13 cells), and (**c**) regular-spiking interneurons (n = 24 cells). The traces shown indicate the most positive voltages at which cells emitted rebound spikes from hyperpolarization offset; traces of cells that did not generate spikes (15/19 pyramidal cells, 10/13 fast-spiking interneurons, and 13/24 non-fast-spiking interneurons) are omitted for clarity. The average current amplitudes (± s.d.) required to elicit at least one rebound spike were 765 ± 526 pA for pyramidal cells (**a**), 800 ± 175 pA for fast-spiking interneurons (**b**), and 431 ± 211 pA for non-fast-spiking interneurons (**c**). Three criteria were used to distinguish fast- from non-fast-spiking neurons: fast-spiking neurons *i*) attained firing rates > 100 Hz during a 500-ms depolarizing current step of 300 ms; *ii*) exhibited a ratio > 0.7 of the average interspike interval (ISI) at the beginning and end of the depolarizing current step (averages of 3 ISIs each); and *iii*) displayed a spike width of ≤ 1ms at half-maximal amplitude. Cells that met all three criteria were classified as fast-spiking (**b**); cells that failed all three criteria as non-fast-spiking (**c**). The "rebound spike thresholds" of pyramidal cells (**a**) and fast-spiking interneurons (**b**) lie around –150 mV, those of non-fast-spiking interneurons (**c**) around -120 mV. One non-fast-spiking interneuron (blue trace in **c**) generated rebound spikes from a hyperpolarization offset of –84 mV, but with spike latency > 100 ms. Any IPSCs triggered by such spikes would have fallen outside our detection window of 5–70 ms after optical stimulus onset (see Supplementary Methods).

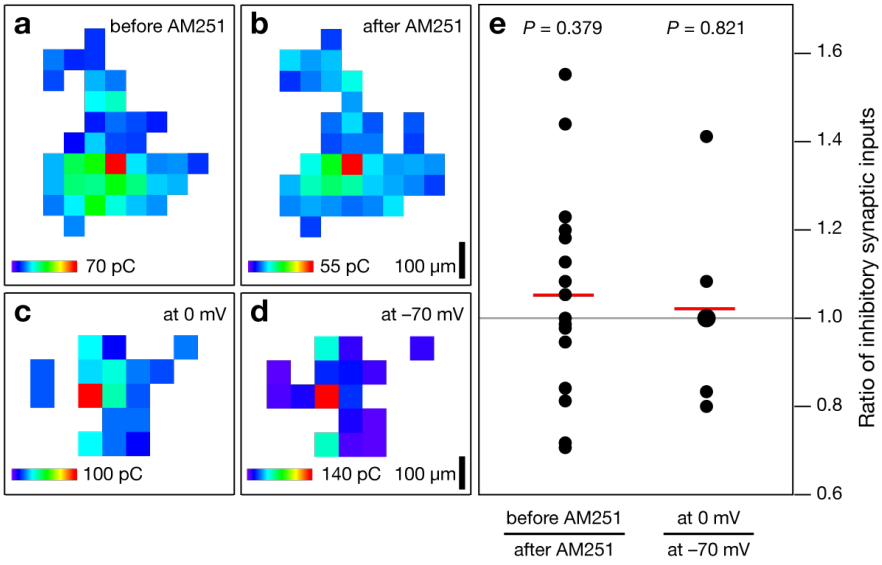

Supplementary Figure 5. Lack of a confound due to depolarization-induced suppression of inhibition (DSI). (**a-d**) Maps of inhibitory inputs to pyramidal neurons in layer 5B. Color on a heat scale symbolizes the charge flowing during the IPSC. To test whether DSI (potentially caused by holding the recorded target neuron at 0 mV) might lead to detection failures of inhibitory inputs, two types of control experiment were performed. (**a**, **b**) In the first type of control experiment, inhibitory input maps were recorded at a holding potential of 0 mV, first in the absence (**a**) and then in the presence of the CB-1 antagonist AM251 (**b**, 2 µM, $n = 17$ cells). (**c**, **d**) In the second type of control experiment, input maps were first recorded at a holding potential of –70 mV (**c**) and subsequently at a holding potential of 0 mV (**d**, $n = 6$ cells). Note that in each case the number and distribution of inhibitory input sources are well-preserved. (**e**) Statistical comparisons of the ratio of inputs detected in each experimental condition in both types of control experiment show no significant deviations from unity (one-sample *t*-test). Each data point represents one cell; population means are indicated by horizontal red lines.

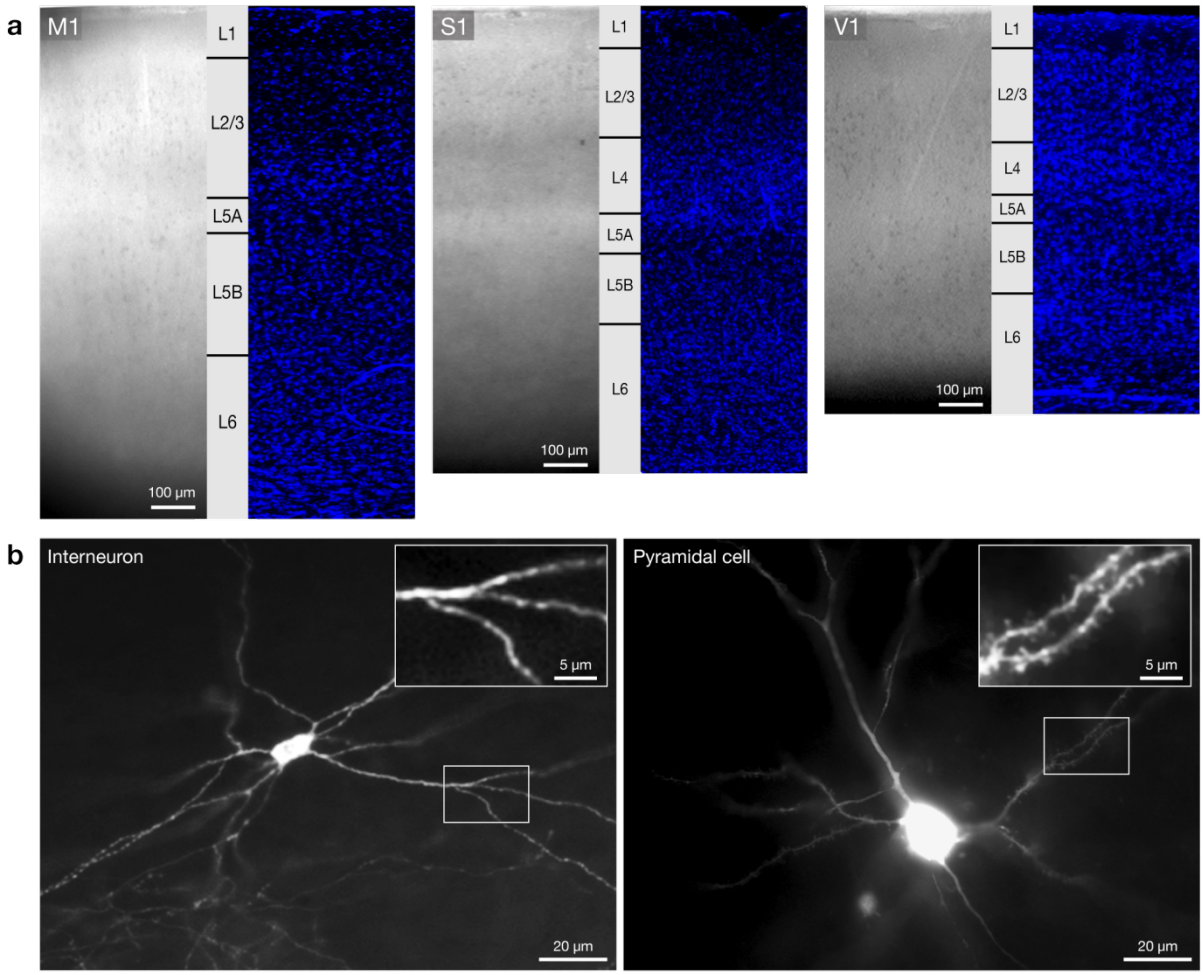

Supplementary Figure 6. Laminar borders and cell morphologies. (a) Slices of primary motor cortex (M1), primary somatosensory cortex (S1), and primary visual cortex (V1) under brightfield (left panels) and epifluorescence illumination highlighting DAPI-stained nuclei (right panels). Left and right panels are from different specimens. (**b**) Wide-field fluorescence images of cells filled with neurobiotin during electrophysiological recordings, followed by fixation and staining with fluorescently labeled streptavidin. Insets reproduce contrast-enhanced images of boxed areas, showing spiny and spineless dendrites of pyramidal cells and interneurons, respectively, at 2.5-fold higher magnification.

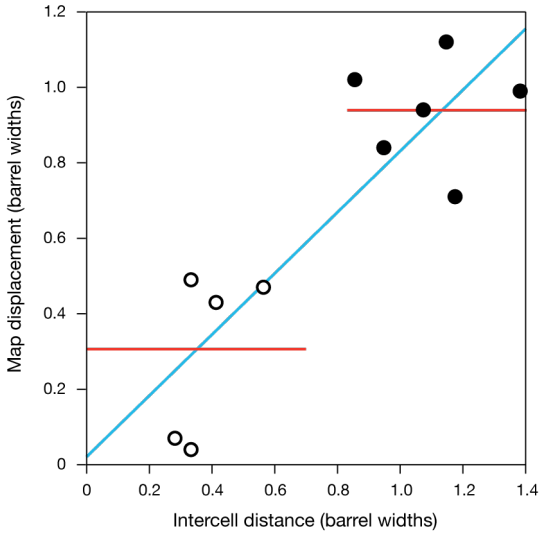

Supplementary Figure 7. Columnar organization of inhibitory inputs. To examine the columnar organization of inhibitory inputs in barrel cortex (S1), we performed paired recordings from layer 2/3 pyramidal neurons located in either the same (open symbols, $n = 5$ pairs) or in adjacent (filled symbols, $n = 6$ pairs) barrel-related columns. The scatterplot shows the tangential displacement between the inhibitory input maps of each cell pair, which was determined by cross-correlation analysis (see Supplementary Methods), as a function of intercell distance. Both measures were normalized by dividing measurements on a μm-scale by the horizontal distances between barrel septa. A step function (red) captures the relationship between intercell distance and map displacement better than a linear fit (blue): the summed squares of residuals (or sums of squares due to error, SSE) are 0.3065 and 0.3601, respectively.

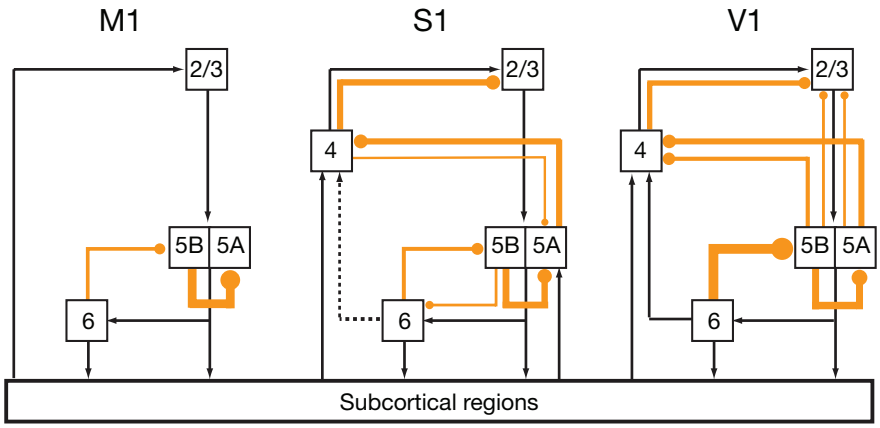

Supplementary Figure 8. Translaminar inhibitory connections (orange, bullet-headed lines) in the context of a "canonical" wiring diagram of excitatory neocortical connections[9] (black, arrow-headed lines). Line thicknesses indicate the strengths of inhibitory connections. Intralaminar connections and translaminar motifs contributing ≤10 % to the total normalized inhibitory charge flow of a target neuron (Fig. 5) were omitted for clarity.

SUPPLEMENTARY TABLES

Supplementary Table 1. Cell-type specificity of ChR2-EGFP expression.

Identifier	Marker	% Coexpression	*n*
Cre	GFP	98.7	234
GFP	Cre	99.5	219
Gad65	GFP	96.4	139
GFP	Gad65	100.0	121
Gad67	GFP	95.1	143
GFP	Gad67	89.7	146
Parvalbumin	GFP	100.0	215
Calretinin	GFP	88.3	196
Calbindin	GFP	89.4	104
Somatostatin	GFP	98.7	151
Neuropeptide Y	GFP	98.0	150
VIP	Cre	94.7	95

Percentages of cells expressing the indicated identifier proteins that also express the indicated marker proteins (*n* = number of cells counted).

Supplementary Table 2. Summary statistics of optical mapping experiments.

	L2/3	L4	L5A	L5B	L6	Sum
M1	9	-	6	9	6	*30*
S1	*22*	8	8	8	8	*54*
V1	15	12	6	12	8	*53*
Sum	*46*	*20*	*20*	*29*	*22*	

Number of excitatory neurons in the indicated cortical areas (rows) and layers (columns) whose inhibitory input distributions were mapped.

Supplementary Table 3. Horizontal (columnar) organization of inhibitory connections.

	M1	S1	V1	*P*-value (ANOVA)
L2/3	302 ± 134 μm	374 ± 104 μm	433 ± 113 μm	0.054
L4	-	284 ± 65 μm	310 ± 121 μm	0.594
L5A	405 ± 61 μm	478 ± 78 μm	303 ± 85 μm	0.002
L5B	553 ± 153 μm	431 ± 99 μm	466 ± 169 μm	0.228
L6	556 ± 97 μm	526 ± 128 μm	399 ± 167 μm	0.109
***P*-value (ANOVA)**	0.002	0.000	0.032	
Significant interlaminar differences ($P < 0.05$)	L2/3 - L5B L2/3 - L6 (L5A - L6)	(L2/3 - L4) (L2/3 - L5A) L2/3 - L6 L4 - L5A L4 - L5B L4 - L6	(L4 - L5B) (L5A - L5B)	

Horizontal distances (means ± s.d.) between the leftmost and the rightmost inhibitory input to an excitatory neuron in the indicated cortical area (columns) and layer (rows). Comparisons of group means by one-way ANOVA revealed only a single significant difference between M1, S1, and V1 (crimson shaded background): the horizontal domain providing input to pyramidal cells in L5A was smaller in V1 than in S1. Within each cortical area, the horizontal spread of inhibitory connections varied significantly from layer to layer (blue shaded background). The pairwise interlaminar differences responsible for the overall intra-areal variation are listed below each column (Tukey-HSD post-hoc test and independent-sample *t*-test; entries in parentheses reached significance levels of $P < 0.05$ only in independent-sample *t*-tests).

Supplementary Table 4. Vertical (laminar) organization of inhibitory connections, as inferred from total laminar charge flow measurements (see Fig. 5).

a Parametric ANOVA

Source layer \ Target layer	2/3	4	5A	5B	6
1	0.167	0.429	0.425	0.509	0.438
2/3	0.000	0.324	0.073	0.948	0.275
4	0.403	0.171	0.039	0.426	0.334
5A	0.003	0.903	0.895	0.340	0.438
5B	0.011	0.039	0.553	0.001	0.136
5	0.001	0.131	0.307	0.001	0.123
6	0.157	0.700	0.376	0.002	0.158

b Non-parametric (Kruskal-Wallis) ANOVA

Source layer \ Target layer	2/3	4	5A	5B	6
1	0.107	0.414	0.323	0.492	0.417
2/3	0.001	0.239	0.017	0.655	0.264
4	0.370	0.105	0.035	0.786	0.317
5A	0.002	0.643	0.945	0.760	0.417
5B	0.055	0.009	0.711	0.002	0.297
5	0.001	0.123	0.393	0.003	0.289
6	0.015	0.804	0.798	0.003	0.295

c Post-hoc analysis of pairwise differences

Comparison of S1 and V1

Source layer \ Target layer	2/3	4	5A	5B	6
1	0.230	0.429	0.881	0.600	0.488
2/3	0.134	0.324	0.582	0.986	1.000
4	0.403	0.171	0.027	0.426	0.334
5A	0.002	0.903	0.913	0.385	0.488
5B	0.008	0.039	0.990	0.022	0.705
5	0.001	0.131	0.586	0.006	0.937
6	0.321	0.700	0.427	0.008	1.000

Comparison of M1 and S1

Source layer \ Target layer	2/3	5A	5B	6
1	0.935	0.632	1.000	1.000
2/3	0.007	0.268	0.988	0.325
4				
5A	0.251	0.999	0.403	1.000
5B	0.752	0.557	0.483	0.116
5	0.371	0.295	0.890	0.127
6	0.743	0.998	0.986	0.204

Comparison of M1 and V1

Source layer \ Target layer	2/3	5A	5B	6
1	0.236	0.406	0.579	0.538
2/3	0.000	0.063	0.943	0.325
4				
5A	0.384	0.908	0.998	0.538
5B	0.177	0.673	0.001	0.383
5	0.137	0.867	0.001	0.218
6	0.165	0.444	0.004	0.196

P-values of comparisons by parametric one-way ANOVA (**a**) or Kruskal-Wallis test (**b**) of differences between M1, S1, and V1 in the amount of inhibitory charge flow from the indicated source layers (rows) to excitatory neurons in the indicated target layers. (**c**) *P*-values of pairwise differences by Tukey-HSD post-hoc test. Significant differences ($P < 0.05$) between cortical areas are highlighted by crimson shaded backgrounds. Data for L4 target cells, which we cannot resolve in M1, were analyzed by independent-sample *t*-test (**a**, **c**) or Mann-Whitney U-Test (**b**).

Supplementary Table 5. Normalized numbers of inhibitory connections.

Target layer		Source layer: 1	2/3	4	5A	5B	6
2/3	M1	9.2 ± 8.9	75.2 ± 15.4	-	8.2 ± 10.1	7.4 ± 8.9	0
	S1	12.8 ± 8.9	47.5 ± 18.3	30.1 ± 18.9	7.0 ± 10.1	5.9 ± 8.6	0.7 ± 1.9
	V1	3.1 ± 4.4	36.5 ± 15.2	27 ± 11.1	13.1 ± 6.8	17.3 ± 15.3	3.0 ± 4.6
4	S1	0	4.1 ± 4.8	58.5 ± 17	31.2 ± 13.2	4.7 ± 7.9	1.6 ± 4.4
	V1	1.2 ± 4.1	2.0 ± 4.2	40.4 ± 20	33.4 ± 10.0	21.9 ± 15.6	1.1 ± 2.7
5A	M1	3.6 ± 4.7	4.0 ± 2.7	-	43.5 ± 17.8	48.4 ± 15.9	1.9 ± 4.5
	S1	1.3 ± 2.6	2.9 ± 4.8	14 ± 9.9	41.9 ± 17.2	37.8 ± 12.6	2.1 ± 3.9
	V1	0	0	3.3 ± 5.1	50.8 ± 29	37.8 ± 18.5	8.1 ± 17.7
5B	M1	0	0.8 ± 2.1	-	5.9 ± 6.5	68.9 ± 10.5	23.8 ± 12.0
	S1	0	1.1 ± 2.3	3 ± 5.5	13.2 ± 18.4	60.0 ± 24.9	22.7 ± 23.3
	V1	0.7 ± 2.5	0.7 ± 2.5	2 ± 2.8	3.9 ± 4.6	42.2 ± 12	50.5 ± 15.6
6	M1	0	0.7 ± 1.7	-	0	2.6 ± 3.1	96.7 ± 4.3
	S1	0	0	0	0	16.9 ± 14.6	83.1 ± 14.6
	V1	3.8 ± 7.5	0	0.9 ± 2.5	0.9 ± 2.5	10.7 ± 11.8	83.7 ± 17.1

Percentages of inhibitory inputs (means ± s.d.) from the indicated source layers to excitatory neurons in the indicated target layers. The table summarizes data from 30 neurons in M1, 54 neurons in S1, and 53 neurons in V1 (Supplementary Table S2). Percentages were obtained by counting the number of inputs from a particular layer and dividing by the cell's total number of identified inputs. Colors indicate significant differences ($P < 0.05$), either between two cortical areas (crimson shaded background) or between one area and the other two (blue shaded background), as determined by parametric and non-parametric one-way ANOVA and subsequent Tukey-HSD post-hoc tests. Data for L4 target cells, which we cannot resolve in M1, were analyzed by independent-sample *t*-test and Mann-Whitney U-Test.

Supplementary Table 6. Absolute numbers of inhibitory connections.

Target layer		Source layer: 1	2/3	4	5A	5B	6
2/3	M1	2.2 ± 1.9	16.4 ± 8.4	-	2.7 ± 3.6	1.2 ± 1.2	0
	S1	1.3 ± 1.6	9.5 ± 3.9	7.3 ± 5.3	2.4 ± 3.7	1.8 ± 3.0	0.2 ± 0.5
	V1	0.8 ± 1.3	9.5 ± 4.9	6.7 ± 2.6	3.3 ± 1.7	5.0 ± 4.9	0.7 ± 1.0
4	S1	0	0.8 ± 0.9	8 ± 3.7	4.6 ± 3.1	0.9 ± 1.5	0.1 ± 0.4
	V1	0.2 ± 0.6	0.3 ± 0.7	6.3 ± 3.5	4.9 ± 1.5	3.9 ± 4.1	0.3 ± 0.9
5A	M1	1 ± 1.3	1.2 ± 1.0	-	12.2 ± 5.5	12.8 ± 3.6	0.7 ± 1.6
	S1	0.6 ± 1.4	1.0 ± 1.6	4.1 ± 3.3	11.6 ± 5.3	11.0 ± 5.5	0.9 ± 1.8
	V1	0	0	0.7 ± 1.0	7.2 ± 1.8	7.7 ± 5.3	2.7 ± 6.1
5B	M1	0	0.4 ± 1.0	-	3.7 ± 4.0	40.2 ± 15.0	16.3 ± 13.4
	S1	0	0.3 ± 0.5	0.8 ± 1.5	3.5 ± 5.8	15.3 ± 7.0	7.8 ± 10.7
	V1	0.3 ± 0.9	0.3 ± 0.9	0.6 ± 0.8	1.2 ± 1.5	11.6 ± 6.1	15.8 ± 10.8
6	M1	0	0.3 ± 0.8	-	0	1.2 ± 1.5	42.3 ± 12.1
	S1	0	0	0	0	6.9 ± 7.7	23.6 ± 11.9
	V1	0.6 ± 1.0	0	0.1 ± 0.4	0.1 ± 0.4	2.4 ± 4.0	13.9 ± 9.1

Numbers of inhibitory inputs (means ± s.d.) from the indicated source layers to excitatory neurons in the indicated target layers. The table summarizes data from 30 neurons in M1, 54 neurons in S1, and 53 neurons in V1 (Supplementary Table S2). Colors indicate significant differences ($P < 0.05$), either between two cortical areas (crimson shaded background) or between one area and the other two (blue shaded background), as determined by parametric and non-parametric one-way ANOVA and subsequent Tukey-HSD post-hoc tests. Data for L4 target cells, which we cannot resolve in M1, were analyzed by independent-sample *t*-test and Mann-Whitney U-Test.

Supplementary Table 7. Charge flow per IPSC.

Target layer		Source layer: 1	2/3	4	5A	5B	6
2/3	M1	14.3 + 13.9	14.7 + 8.5	-	16.1 + 14.2	12.3 + 7.3	0
	S1	18.6 + 12.9	29.1 + 21.1	27.1 + 21.8	12.0 + 7.4	12.8 + 8.2	12.8 + 8.2
	V1	5.6 + 7.0	10.6 + 6.5	13.4 + 17.8	14.1 + 19.7	10.2 + 9.0	10.0 + 4.4
4	S1	-	27.1 + 19.8	41.8 + 27.0	37.2 + 18.2	11.1 + 6.4	21
	V1	-	13.4 + 5.9	17.3 + 17.6	18.9 + 29.3	13.7 + 15.4	5.1 + 0.4
5A	M1	10.4 + 15.2	8.4 + 7.5	-	13.8 + 4.8	14.1 + 10.8	4
	S1	15.2 + 7.1	16.0 + 7.7	31.4 + 12.6	53.7 + 27.2	44.4 + 30.1	18.7 + 5.4
	V1	0	0	6.5 + 4.3	17.4 + 13.9	11.7 + 6.8	5.3 + 0.3
5B	M1	0	7.3 + 2.5	-	9.4 + 4.8	21.2 + 7.7	15.2 + 6.7
	S1	0	6.6 + 1.4	13.4 + 1.6	15.8 + 9.3	26.9 + 15.4	15.3 + 15.0
	V1	7.1	8.1	5.3 + 2.9	8.1 + 4.6	10.1 + 4.7	10.5 + 6.4
6	M1	2	0	-	0	6.3 + 3.1	7.4 + 2.8
	S1	0	0	0	0	13.7 + 11.3	14.3 + 10.5
	V1	0.8 + 1.4	0	0	0	6.3 + 3.3	7.4 + 3.8

Average charge flow per IPSC in pC (means ± s.d.) from the indicated source layers to excitatory neurons in the indicated target layers. The table summarizes data from 30 neurons in M1, 54 neurons in S1, and 53 neurons in V1 (Supplementary Table S2). Colors indicate significant differences ($P < 0.05$), either between two cortical areas (crimson shaded background) or between one area and the other two (blue shaded background), as determined by parametric and non-parametric one-way ANOVA and subsequent Tukey-HSD post-hoc tests. Data for L4 target cells, which we cannot resolve in M1, were analyzed by independent-sample *t*-test and Mann-Whitney U-Test.

Supplementary Table 8. Classification of excitatory neurons by their inhibitory input patterns (see Fig. 6a).

a Charge flow (%)		Target layer				
		L2/3	L4	L5A	L5B	L6
P-value	Y1	0.000	0.292	0.017	0.021	0.251
	Y2	0.003	-	0.2	0.438	0.462
Correct prediction	M1	100.00%	-	100.00%	89.00%	83.30%
	S1	68.00%	87.50%	62.50%	25.00%	62.50%
	V1	73.00%	75.00%	83.30%	75.00%	12.50%
	Mean	76.10%	80.00%	80.00%	65.50%	50.00%
Incorrect prediction	M1	0%	-	0%	11% V1	16.7% V1
	S1	18% M1 14% V1	12.5% V1	37.5% V1	37.5% M1 37.5% V1	37.5% M1
	V1	7% M1 20% S1	25% S1	16.7% S1	8.3% M1 16.7% S1	50% M1 37.5% S1

b Number of inputs (%)		Target layer				
		L2/3	L4	L5A	L5B	L6
P-value	Y1	0.000	0.134	0.047	0.042	0.139
	Y2	0.019	-	0.141	0.415	0.141
Correct prediction	M1	100%	-	100%	100%	100%
	S1	60%	87.50%	62.50%	25%	62%
	V1	80%	83.30%	100%	83.30%	37.50%
	Mean	73.80%	85%	85%	72.40%	63.60%
Incorrect prediction	M1	0%	-	0%	0%	0%
	S1	20% M1 20% V1	12.5% V1	12.5% M1 25% V1	37.5% M1 37.5% V1	37.5% M1
	V1	20% S1	16.7% S1	0%	16.7% M1	50% M1 12.5% S1

Discriminant functions were constructed to examine whether the overall laminar source distributions of inhibitory inputs to excitatory neurons in different target layers differed among cortical areas M1, S1, and V1 (Fig. 6a). Discriminance functions take the form of linear combinations: $Y = b_0 + b_1 * X_1 ... + b_n * X_n$, rendering a certain discriminant variable Y from predictor variables X_1 to X_n. in dependence of discriminant coefficients b_i. Here, these functions incorporated as predictor variables X the total laminar inhibitory charge flows (**a,**

see Fig. 5) or input counts (**b**; see Supplementary Table 5) from all cortical layers but L4 (which we cannot resolve in M1), and hence, produce a discriminant variable Y_j for every individual cell j.

Arithmetic means (centroids, Y_C) and standard deviations (S) over Y_j are calculat ed within each of the three groups (cortices, Y_{Cw}, S_w) as well as between Y_{Cb}, S_b). Discriminant coefficients b_i are optimized with respect to a minimal ratio of between-goup-to-within-group variance (S_b/S_w), resulting in the following discriminant functions:

For L2/3: $Y1 = 0.09\ L1 + 1.32\ L2/3 + 0.87\ L5A + 0.34\ L5B - 0.27\ L6$
$Y2 = -0.13\ L1 - 0.03\ L2/3 + 0.58\ L5A + 0.49\ L5B + 0.43\ L6$

For L5A: $Y1 = 0.65\ L1 + 1.28\ L2/3 + 3.07\ L5A + 2.81\ L5B + 0.84\ L6$
$Y2 = -0.11\ L1 - 0.28\ L2/3 + 1.88\ L5A + 1.34\ L5B + 1.22\ L6$

For L5B: $Y1 = 1.43\ L1 - 1.03\ L2/3 + 1.25\ L5A + 0.7\ L5B + 1.88\ L6$
$Y2 = -0.10\ L1 + 1.74\ L2/3 + 3.26\ L5A + 6.67\ L5B + 7.6\ L6$

P-valus for significance tests comparing the means (centroids) of the discriminant values Y1 and Y2 for excitatory neurons in M1, S1, and V1, were calculated to estimate, if cortices could be successfully separated by the retrieved functions. P-values are tabled for the indicated layers (crimson backgrounds indicate $P < 0.05$). Percentages of correct and incorrect predictions are given below.

Supplementary Table 9. Abundance of interneuron subtypes.

	Layer	Cells per 0.05 mm^3			*P*-value				*n*		
		M1	S1	V1	ANOVA	M1-S1	M1-V1	S1-V1	M1	S1	V1
PV	4	-	611 ± 106	525 ± 115	-	-	-	0.021	-	18	22
	5B	309 ± 84	430 ± 71	419 ± 97	0.000	0.000	0.001	0.925	21	16	18
	6	132 ± 32	207 ± 111	184 ± 59	0.025	0.024	0.163	0.732	23	17	16
SOM	4	-	116 ± 43	188 ± 47	-	-	-	0.000	-	13	14
	5B	130 ± 44	175 ± 64	168 ± 68	0.043	0.050	0.110	0.921	20	21	22
	6	91 ± 46	93 ± 54	74 ± 27	0.308	0.988	0.430	0.339	20	21	21
VIP	4	-	109 ± 63	139 ± 67	-	-	-	0.198	-	18	15
	5B	79 ± 29	71 ± 34	79 ± 50	0.841	0.870	0.999	0.873	12	13	9
	6	93 ± 26	71 ± 37	63 ± 29	0.125	0.234	0.150	0.859	11	13	7

Neocortical slices were obtained from *Gad2::Cre-ER^{T2} R26::ChR2-EGFP* mice 1–7 days after tamoxifen induction and immunolabeled with antibodies against GFP plus parvalbumin (PV), somatostatin (SOM), and vasoactive intestinal peptide (VIP), respectively. Numbers of PV-, SOM-, and VIP-positive interneurons were determined in image stacks of n 50 μm-thick slices; cell counts are reported as cells per 0.05 mm^3 (means ± s.d.). Crimson shaded backgrounds indicate significant differences ($P < 0.05$) between two cortical areas, as determined by parametric one-way ANOVA and subsequent Tukey-HSD post-hoc tests. Data for L4 target cells, which we cannot resolve in M1, were analyzed by independent-sample t-test.

Supplementary Table 10. Transmission failure rates.

Connection		Transmission failure rate			*P*-value			
Source	Target	M1	S1	V1	ANOVA	M1-S1	M1-V1	S1-V1
2/3	2/3	0.31 ± 0.10	0.30 ± 0.11	0.28 ± 0.15	0.918			
5A	2/3	0.33 ± 0.11	0.34 ± 0.11	0.33 ± 0.18	0.593			
5B	2/3	0.43 ± 0.13	0.33 ± 0.16	0.37 ± 0.20	0.946			
4	4	-	0.45 ± 0.06	0.28 ± 0.15	0.004	-	-	0.004
5B	4	-	0.43 ± 0.18	0.32 ± 0.09	0.150			
5A	5A	0.27 ±0.18	0.23 ± 0.12	0.25 ± 0.13	0.821			
4	5A	-	0.42 ± 0.06	0.32 ± 0.15	0.162			
5B	5B	0.22 ± 0.07	0.27 ± 0.10	0.34 ± 0.13	0.046	0.557	0.038	0.349
6	5B	0.39 ± 0.09	0.38 ± 0.15	0.30 ± 0.19	0.401			

Failure rates of IPSCs from the indicated source layers onto excitatory postsynaptic cells in the indicated target layers (means ± s.d.). The table only includes inhibitory circuit motifs with characteristic area-specific differences (Fig. 5). Failure rates were estimated as the fraction of optical stimuli which failed to elicit supra-threshold IPSCs (see Supplementary Methods). Because no significant area-specific differences in optical responsiveness were detected (Supplementary Fig. 2), differences reflect predominantly synaptic transmission failure rates. Crimson shaded backgrounds indicate significant differences ($P < 0.05$) between two cortical areas, as determined by parametric one-way ANOVA and subsequent Tukey-HSD post-hoc tests. Data for L4 target cells, which we cannot resolve in M1, were analyzed by independent-sample *t*-test.

Supplementary Table 11. IPSC rise times.

Connection		20–80 % rise time (ms)			*P*-value			
Source	Target	M1	S1	V1	ANOVA	M1-S1	M1-V1	S1-V1
2/3	2/3	9.0 ± 2.4	6.9 ± 2.3	6.2 ± 2.1	0.037	0.255	0.029	0.304
5A	2/3	10.3 ± 5.5	6.7 ± 2.7	7.5 ± 2.4	0.215			
5B	2/3	11.0 ± 3.5	6.6 ± 2.1	8.3 ± 2.0	0.113			
4	4	-	5.6 ± 1.3	7.5 ± 2.8	0.094	-	-	
5B	4	-	4.8 ± 3.2	8.8 ± 1.6	0.008	-	-	0.008
5A	5A	10.7 ± 2.9	5.8 ± 1.2	5.3 ± 1.7	0.000	0.000	0.000	0.884
4	5A	-	5.7 ± 1.1	7.5 ± 1.4	0.063	-	-	
5B	5B	5.7 ± 1.6	5.2 ± 1.2	5.9 ± 1.4	0.665			
6	5B	8.4 ± 2.3	4.8 ± 1.3	5.4 ± 2.0	0.004	0.009	0.01	0.731

IPSC rise times from the indicated source layers onto excitatory postsynaptic cells in the indicated target layers (means ± s.d.). Rise times were measured for single IPSCs on individual trials and represent the interval between the rising IPSC reaching 20 % and 80 % of its maximal amplitude. The table only includes inhibitory circuit motifs with characteristic area-specific differences (Fig. 5). Crimson shaded backgrounds indicate significant differences ($P < 0.05$) between two cortical areas, as determined by parametric one-way ANOVA and subsequent Tukey-HSD post-hoc tests. Data for L4 target cells, which we cannot resolve in M1, were analyzed by independent-sample *t*-test.